THE ASTRONOMICAL JOURNAL VOLUME 102, NUMBER 1 JULY 1991

SHORT TIMESCALE BROAD EMISSION-LINE FLUX VARIABILITY IN HIGH-LUMINOSITY ACTIVE GALACTIC NUCLEI

Kirk T. Korista[1]
Department of Astronomy, The Ohio State University, Columbus, Ohio 43210
Received 6 September 1990; revised 11 March 1991

ABSTRACT

The standard model of AGN suggests that the broad-line regions of high-luminosity AGN should be so large that any variability in the broad emission-line fluxes should be on timescales of ~2–4 yr or more. Spectrophotometric observations of eight radio-quiet QSOs over a period of 1 yr revealed definite Hβ flux variability in one of these objects and possibly in two others. This may be an indication that the BLRs in high-luminosity AGNs are much smaller than those predicted by the standard model, as is apparently the case in Seyfert galaxies.

1. INTRODUCTION

Because the broad emission-line regions in high-luminosity active galactic nuclei (HLAGN), or quasistellar objects (QSOs), were thought to be very large, little or no variability in the broad emission lines was expected. However, reports of significant broad emission-line variability in HLAGN on timescales of less than ~1 yr started to appear in the literature in 1986 (Gondhalekar *et al.* 1986; Zheng & Burbidge 1986). Since then further reports have been made (Zheng *et al.* 1987; Gondhalekar 1987; O'Brien *et al.* 1989; Perez *et al.* 1989; Gondhalekar 1990), and the strong possibility of such variability in HLAGN can no longer be ignored. Here we describe a study undertaken to see if broad emission-line flux variations in HLAGN on these short timescales could be confirmed. In Sec. 2 we describe the observations. We present the results in Sec. 3 and a discussion and summary follows in Sec. 4.

2. THE OBSERVATIONAL PROGRAM

2.1 The Program Goals

A relatively large sample of QSOs were to be systematically observed spectrophotometrically at predetermined intervals on timescales of 1 yr and less. QSOs have been observed in this way for broad emission-line variability only once before (Perez *et al.* 1989) for a sample of six *radio-loud* QSOs. Here 12 *radio-quiet* QSOs were chosen to be observed on two separate timescales: 2–3 months and 9–12 months. It was not our intention to determine the size of the BLRs of QSOs, rather this was to be a preliminary investigation into determining whether the broad emission lines of high luminosity AGN (HLAGN) do indeed vary on timescales of ~1 yr or less as had been recently reported (however, note that continuum variations in QSOs have been known for ~25 yr). With a relatively large number in the sample (12) we also wanted to establish just how prevalent the short timescale broad emission-line variability in HLAGN is.

We wanted to acquire higher quality data than that upon which most other reports of HLAGN broad emission-line variability were based, with convincing results at some reasonably low level of variability (~15%). This kind of data is attainable with the Ohio State University CCD spectrograph on the 1.8 m Perkins telescope of the Ohio State University and Ohio Wesleyan University at the Lowell Observatory, and using a nearby constant narrow line for internal flux calibration. This program has the advantage over earlier studies in one or more of the following ways: (1) the data are of higher signal to noise; (2) we do not need to rely on absolute spectrophotometry; we require only relative fluxes calibrated internally with a nearby constant narrow line; (3) the QSOs are systematically sampled on predetermined timescales.

However, a few setbacks occurred in the implementation of the then newly built CCD spectrograph, and the program had to be scaled back due to time constraints. Fewer objects (8) were observed less frequently. Only five objects were observed on timescales of 2–3 months and five objects on the timescale of 9–12 months, including an Image Dissector Scanner (IDS) observation made in the Autumn of 1987. Note that not all of the 8 objects were observed on each timescale. However, any discovery of broad emission-line variations would be significant, and the project went forth as described below.

We chose to observe the broad Balmer emission line Hβ λ 4861 for the following reasons. In order to put all of the data from each object on the same flux scale (in general they will not be on the same scale due to the grey extinction of clouds), we scale the data to the flux of the nearby forbidden [O III] λ 5007 line, which is not expected to vary on the timescales of interest. Without this scaling capability made available by the nearby constant [O III] line, we would have to rely on acquiring absolute instead of relative spectrophotometry. This is the most important reason for our choice of broad emission line. The last two reasons are more incidental: Hβ is a relatively strong broad emission line, and with the available instrumentation we could in principle observe it in QSOs of redshifts just under 1.0, giving us a large number of QSOs from which to choose.

2.2 QSO Selection Criteria

High-luminosity AGN have a wide range in observed characteristics. Those of common traits are often put into their own category, such as: radio-quiet QSOs, radio-loud (steep and flat spectrum) QSOs, blazars [BL-Lac objects, optically violently variable QSOs (OVVQs), and high polar-

[1] Present address: The Observatories of the Carnegie Institution of Washington, 813 Santa Barbara Street, Pasadena, CA 91101.

ization QSOs (HPQs)], and broad absorption line QSOs (BALQSOs). In addition they also come with a variety of brightnesses, apparent and intrinsic. To optimize the quality of the data and to constrain as much as possible the range in interpretations of the results, the sample of QSOs in this study was carefully chosen from Hewitt & Burbidge (1987) according to the selection criteria described below:

Luminosity. All AGN in this study are brighter than $M_B = -22.1$ (for $H_0 = 75$ km s^{-1} Mpc^{-1} and $q_0 = 0.5$), which defines the distinction (real or not) between Seyfert 1 galaxies and QSOs (see, for example, Osterbrock 1988).

Apparent Magnitude. The QSOs in the sample were required to have apparent magnitudes brighter than 17 mag in order to acquire a desirable signal to noise in a reasonable integration time ($\leqslant 2$ hr).

QSO Redshift. As stated above we may observe Hβ, [O III] λ 5007 and some surrounding continuum in those QSOs with $z < 1.0$. However, in order to avoid the telluric absorption bands and the OH sky emission bands, we restricted the redshifts to $z \leqslant 0.34$.

[O II] and Fe II Emission. In order to put the spectra on the same flux scale, we must measure the [O III] λ 5007 flux with reasonable accuracy. Thus we avoided those QSOs with weak [O III] λ 5007. In addition we wanted to avoid those QSOs with strong broad permitted Fe II emission, which in the form of (m42) $\lambda\lambda$ 4924,5018 (and other multiplets as well) often muddles the spectrum near the red wing of Hβ, significantly contaminating the [O III] lines, while the Fe II λ 4570 and λ 5250 blends can confuse the placement of the continuum near Hβ. Both criteria were checked through a literature search for previously published spectra. In summary we wanted to avoid the problems associated with [O III] flux calibration when the contrast between [O III] and the underlying Fe II is small (see, for example, Baribaud & Alloin 1990).

Radio Properties. We required the QSOs in our sample to be radio quiet, in contrast to the monitoring program of Perez *et al.* (1989) in which all the objects were radio loud. This means we excluded radio selected objects (3C, 4C, and PKS objects), and additionally BL-Lac objects, HPQs, and OVVQs. All of these type of QSOs are thought to have at least some fraction of their observable continua beamed (in many cases along or near our line of sight), while there is no evidence for continuum beaming in radio-quiet QSOs. If a significant fraction of the exciting continuum is beamed, then the light curves of the variable continuum and the variable broad emission lines tell us nothing about the size and little about the structure of the BLR in HLAGN, which are ultimately the questions we want to answer. All but four in our (original) sample of 12 are ultraviolet excess objects (PG and US surveys), three are x-ray selected objects, the last an NAB object (a QSO found lying in the direction of an Abell cluster). All are radio quiet.

2.3 Observations and Data Reduction

Most of the observations presented here were obtained with the Ohio State University CCD spectrograph on the 1.8 m Perkins telescope of the Ohio State University and Ohio Wesleyan University at the Lowell Observatory. The CCD is a Texas Instruments 4849 400×580 chip, and it is mounted on a Boller and Chivens spectrograph. The 350 lines per millimeter grating used (at first order) has 1100 Å coverage, and when coupled with a 5 arcsec slit width, results in a spectral resolution of 9 Å. The wide slit was employed to ensure that most or all of the light fell into the slit, even on nights of fair or poor seeing. Typical seeing was 2–3 arcsec, although one night (JD 2447848) the seeing varied between 3 and 5 arcsec. Because of the large distances of these objects, it was not expected that aperture effects, due to the interplay of guiding/seeing effects and extended [O III] often observed in Seyfert galaxies, would be a problem in this study. However, to be absolutely certain the large 5″ slit was used. Sky conditions were generally clear with thin cirrus; only one night (JD 2447573) was deemed to be photometric. Individual exposure integration times were 1800 s, and usually 3–4 exposures were taken per object. This resulted in signal-to-noise ratios of typically 40–65, although a couple observations were in the 20–30 range (e.g., 1E0357 + 107). An order separating filter was used when necessary to block out second-order blue light. A log of the observations is given in Table 1. The object name, redshift, the Julian Date of observation, the total integration time, and the instrument used are listed in columns 1–5, respectively.

The CCD data were reduced in the usual way with IRAF. Every CCD frame contained a 20 ms preflash which, along with the bias level, was subtracted from the data. Several quartz lamp exposures were taken for every grating setting to remove the CCD pixel-to-pixel variations. One to two iron-neon lamp and standard star exposures were taken per object per night to wavelength and flux calibrate the extracted spectra. All program objects, including standard stars, were observed along the same column on the CCD chip. This column (± few pixels) corresponds to the center of the chip where the slit illumination profile is relatively constant for ~100 pixels on either side. Thus no sky flats were necessary to determine the slit illumination profile. The background was carefully fitted along either side of the object and subtracted off during the extraction of the data to one dimension.

A few of the observations were obtained with the Ohio State University Image-Dissector Scanner (IDS) (Byard *et*

TABLE 1. Log of observations.

QSO (1)	z (2)	Julian Date (3)	Integration Times(s) (4)	Instrument (5)
PG0026+129	0.142	4553	1600	IDS
		7413	3600	IDS
		7778	5400	CCDsp
		7848	5400	CCDsp
PG0052+251	0.155	7778	5400	CCDsp
		7847	5400	CCDsp
PG0157+001	0.163	7788	5400	CCDsp
		7848	7200	CCDsp
NAB0205+024	0.155	4553	1600	IDS
		7783	5400	CCDsp
		7847	5400	CCDsp
1E0357+107	0.182	7572	5400	CCDsp
		7848	7200	CCDsp
1E0514-005	0.292	7560	5400	CCDsp
		7573	7200	CCDsp
		7849	7200	CCDsp
0833+446	0.255	7534	3600	CCDsp
		7560	7200	CCDsp
		7572	5400	CCDsp
		7849	7200	CCDsp
PG0906+484	0.118	7571	5400	CCDsp
		7572	5400	CCDsp
		7573	7200	CCDsp
		7848	7200	CCDsp
		7915	7200	CCDsp

al. 1981) on the same telescope with 7 arcsec circular entrance apertures and reduced as described by Peterson (1987). These data are from the OSU IDS data archive, and were not part of the observing program outlined above. However, these data could be used to investigate variability on longer timescales, and one of the three IDS observations was taken (PG0026 + 129: by the author) only 1 year prior to the first CCD observation of PG0026 + 129. These data are also listed in Table 1.

3. THE RESULTS

3.1 Measurements

As discussed above all data for each QSO were scaled to the same flux in [O III] λ 5007. In addition difference spectra were formed for each QSO dataset, and the residual was checked for any evidence of the [O III] lines. In all cases [O III] λ 5007 is contaminated with Fe II (m42) λ 5018; however, the contamination is weak as these objects were selected against strong optical Fe II emission. In all cases the chosen flux scales resulted in minimum [O III] residual, demonstrating that weak Fe II did not confuse the flux measurement of the [O III] λ 5007 line (to the level of accuracy that we are looking for, namely, better than $\sim 10\%$). One must keep in mind that we do not require the absolute flux of [O III], and in general the contamination of the broad Fe II would lead us to underestimate the broad emission-line variability. We found that the relative scaling between spectra, based upon the constancy of the [O III] flux, was good to $\sim 8\%$ for 1E0357 + 107 and $\sim 4\%$ for the remainder of the QSOs observed. That is, if the relative scale factor differed from that chosen by more than this amount, one could begin to detect residual [O III] emission.

The estimated flux measurement errors are 9.8% for 1E0357 – 007 and about 5.8% for the remainder of the objects. The flux measurement errors for the IDS data were estimated to be 8%–10%. One may assess the significance of any variation in the broad emission line or continuum by comparing the flux differences with their estimated 1σ measurement errors (here we assume that our flux measurement errors are Gaussian distributed), as well as by looking at Figs. 1–8 (see below) in which the "difference" spectra are plotted just below the "parent" spectra. From these difference spectra one may judge the following: (1) how well the flux scales in the parent spectra were set by looking for residual [O III] emission, and (2) the extent to the variation in broad Hβ compared to the nearby "continuum," if any (note, however, that in the spectral region shown in Figs. 1–8, very few pixels, if any, are strictly emission-line free). It is the very significant ($>3\sigma$) flux variations that we are especially interested in to confirm the short timescale broad line flux variability in HLAGN. This type of variation would also be required in future studies to determine the sizes of the BLRs in QSOs. However, we considered those flux variations at better than the 2σ level to be suggestive of true variations and are thus included in the tables and discussion. Finally, those variations below the 2σ level are mentioned for completeness, but are given very little weight.

To set and measure the continuum a straight line was drawn between about 4750 and 5100 Å; these endpoints are relatively free of emission lines. So as to not introduce more noise and sources of error, the two narrow lines of [O III] and the broad Fe II were not subtracted from the region near the red wing of Hβ. Instead, all broad Hβ line fluxes were consistently measured between 4750 and 4950 Å, just blueward of the narrow line [O III] λ 4959. This measurement includes the constant but very weak narrow-line Hβ, Fe II (m42) λ 4924 and possibly other multiplets of Fe II (Joly 1988). Permitted Fe II is known to vary with the broad emission lines, but the optical multiplets may vary with a lower amplitude (Wamsteker *et al.* 1990). If the nearby Fe II does vary with a lower amplitude, then this would again result in an underestimate of broad Hβ variability. However, the weakness of the Fe II in all of the spectra guarantees that λ 4924 did not confuse the measurement of broad Hβ. Missing from this measurement are the extreme red wings of Hβ, containing very little ($\sim 7\%$) of the total line flux.

3.2 Individual Results

Of the eight QSOs observed, two showed evidence for broad emission-line variability (PG0026 + 129, 1E0357 + 107) at the $>2\sigma$ level, and one at better than the 3σ level (1E0514 – 005). Two others (0833 + 446 and PG0052 + 251) varied marginally, with variations at the 1.9σ and 1.4σ levels, respectively. Not even continuum variations were observed in the other QSOs. Table 2 outlines, for those QSOs which varied at the 2σ level or better, the (rest frame) broad emission line and continuum fluxes and equivalent widths. The time intervals between observations were binned into the two groups discussed earlier: 2–3 months and 9–12 months. In addition, multiple CCD observations and some IDS data allowed us to check for variability in a few objects on timescales of 2–4 weeks and 8–9 yr. The binned time interval between observations, the number of QSOs observed in the binned time interval, the number of pairs of observations per time interval, the number of pairs that showed broad line variability ($>2\sigma$) during a given time interval, and which QSOs were observed to vary on that timescale are shown in columns 1–5 of Table 3, respectively. An observation pair has been defined to mean two consecutive observations. Figures 1–5 show examples of (rest frame) spectra of the nonvarying, or marginally varying ($<2\sigma$), QSOs and their differences, while Figs. 6–8 show the same for the three significantly varying ($>2\sigma$) QSOs. CCD observations that were compared with the IDS data

TABLE 2. Rest frame continuum and Hβ fluxes for the varying QSOs.

QSO (1)	Julian Date (2440000+) (2)	F_λ[a] (5000Å) (3)	F(Hβ)[b] (4)	W_λ(Å) (5)
PG0026+129	4553	3.59±0.29	2.27±0.18	60.0
	7413	2.99±0.24	2.00±0.16	64.8
	7778	3.15±0.18	1.68±0.10	50.1
	7848	2.97±0.17	1.93±0.11	63.0
1E0357+107	7572	1.23±0.12	1.30±0.13	105.1
	7848	1.75±0.17	1.64±0.16	90.6
1E0514-005	7573	2.61±0.15	2.28±0.13	81.6
	7849	3.27±0.19	2.82±0.16	79.6

[a]: in units of 10^{-15} ergs s^{-1} cm^{-2} Å^{-1}

[b]: in units of 10^{-13} ergs s^{-1} cm^{-2}

[c]: for continuum and line variations, respectively.

TABLE 3. The distribution of QSO observations and broad line variability.

t_{BIN} (1)	Number of QSOs observed per bin (2)	Number of Pairs of Observations (3)	Number of Pairs that Varied (4)	Which QSOs Varied (5)
2 - 4 weeks	2	3	0	-
2 - 3 months	5	5	0-1	PG0026+129
9 - 12 months	5	5	1-3	1E0514-005 1E0357+107 PG0026+129
8 - 9 years	2	2	0	-

Total Number of QSOs Observed: 8

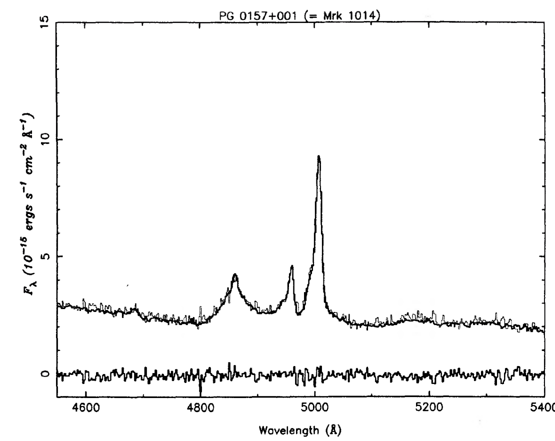

FIG. 2. The same as Fig. 1 for PG0157 + 001 (= Mrk 1014) (JD 2447788 light, JD 2447848 heavy). Note the strongly blue asymmetric [O III] lines.

were smoothed to the IDS resolution in each case. Below we discuss the individual results for the observed QSOs.

3.2.1 PG0052+251

Figure 1 shows variations in the broad Hβ flux at the 8% level and in the continuum at the 7% level over the time interval of $\Delta t = 69$ days. The excess emission in JD 2447778 near 4850 and 4876 Å (rest frame) are apparently not spurious, as they appear in every exposure for that night. The nearest night sky line lies 21 Å blueward of the blue excess, and we do not believe them to be artifacts of the division by the flatfield. However, whether these represent a true profile variation and thus a change in the line flux is difficult to say. The broad emission line and continuum varied at the 1.4σ and 1.1σ levels, respectively, and are thus taken to be marginal detections of variability.

3.2.2 PG0157+001 (=Mrk 1014)

The continuum and broad line flux levels are the same in both observations, separated by 60 days, the only observational pair for this QSO (see Fig. 2). Note in Fig. 2 the [O III] profiles have a fairly strong blue asymmetry. The "blue" feature is real as it appears in both spectra, and it is almost certainly [O III] since the blue asymmetry has the correct flux ratio of 3:1. Blue asymmetries in narrow lines are common in Seyfert and radio galaxies (Heckman *et al.* 1981). Direct imaging (Heckman *et al.* 1984; MacKenty & Stockton 1984; Smith *et al.* 1986; Stockman & MacKenty 1987) has shown a large ($\sim$90 kpc) extended spiral-like continuum emission region surrounding the nucleus, but little if any extended [O III]. In any case the ratio of the blue to the main component remained constant between the two spectra. We are therefore confident that the secondary (blue) component did not affect our ability to accurately place both observations on the same flux scale.

3.2.3 NAB0205+024

No continuum or broad emission line variations were detected between JD 2447783 and JD 2447847 (see Fig. 3). Another observation made with the IDS taken $\sim$9 yr prior is identical to the above two spectra.

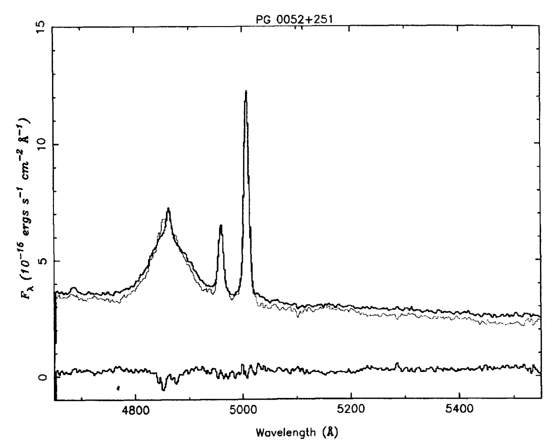

FIG. 1. The two observations of Hβ PG0052 + 251 (JD 2447778 light, JD 2447848 heavy) and their difference (lower heavy = JD 2447848–JD 2447778). All difference spectra in the figures that follow are the later date minus the earlier.

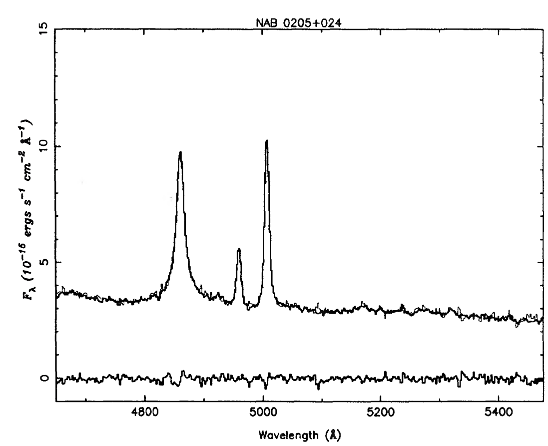

FIG. 3. The same as Fig. 1 for NAB0205 + 024 (JD 2447783 light, JD2447847 heavy).

1991AJ....102...41K

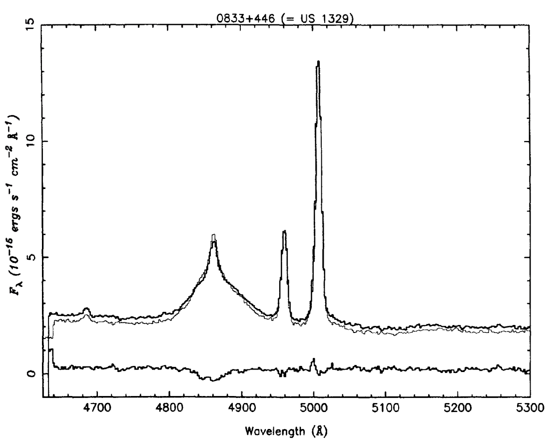

FIG. 4. The same as Fig. 1 for 0833 + 446 (= US1329) (mean of JD 2447572,7560,7534 light, JD 2447849 heavy).

3.2.4 0833 + 446 (= US1329)

Observations separated by 26 days (JD 2447534 and JD 2447560) and 12 days (2447560 and 2447572) show no variation and are all identical. A mean of these three spectra was then compared to one taken 277 days later (JD 2447849). Figure 4 shows a -11% change in the broad Hβ flux and $+11.6\%$ change in the continuum over the latter period. These are 1.9σ and 1.8σ variations, respectively, and thus were considered to be marginal.

3.2.5 PG0906 + 484

Those observations of this QSO taken on JD 2447571, 2447572, and 2447573 were averaged and compared to that taken on JD 2447848 ($\Delta t = 275$ days), and the latter was then compared to 2447915 ($\Delta t = 67$ days). No variations in continuum or broad emission line fluxes were detectable in either case (see Fig. 5).

3.2.6 PG0026 + 129

Significant variations in both the broad emission line and the continuum on short timescales have, apparently, been observed before for this object: 10 months (Zheng *et al.* 1987) and 12 months, based on broad Hβ/[O III] flux ratio comparisons between data from Peterson *et al.* (1981) and Shuder (1984). Table 2 and Fig. 6 show that the broad Hβ flux decreased (-16%) between JD 2447413 and JD 2447778 (365 days) and then returned ($+15\%$) to the JD 2447413 level by JD 2447848 (70 days). These variations occurred at the 2–2.3σ level. The night sky line of [O I] λ 5577 falls on the red side of the core of Hβ (near 4872 Å). However, Fig. 6 shows that most of the variation occurred, or at least most of the residual flux lies, blueward of where the sky line falls. It is clear that the residual broad emission flux in Fig. 6 is not due to imperfect removal of this night sky line in any of the spectra. The continuum was essentially at the same level during all three observations. If the broad emission-line variation is real, then the continuum must have changed twice (decrease and then increase) sometime in the past, perhaps between JD 2447413 and JD 2447778. These short timescale variations are important if they are indeed real; a 70 day variation of the broad emission-line flux would be one of the shortest ever measured for this luminosity class. A 2.1σ continuum change (-17%) and a 1.5σ broad emission-line flux change (-13%) also occurred over the long time interval between JD 2444553 and JD 2447413, the latter deemed a marginal detection of variability.

3.2.7 1E0357 + 107

This QSO has not been observed to the extent of PG0026 + 129. There have been no previous reports of continuum or broad emission-line flux variations in this object. However, we have detected a very significant (3.1σ level) change in the continuum at 5000 Å ($+44\%$) and a 2.1σ level change in the broad Hβ flux ($+26\%$) between JD 2447572 and JD 2447848 (276 days) (Refer to Table 2 and Fig. 7). No night sky lines of any significance fall anywhere near the Hβ region.

3.2.8 1E0514 − 005

There are no previous reports of broad emission-line variability in this QSO. The first two observations, JD 2447560 and JD 2447573 ($\Delta t = 13$ days) were identical, and averaged together. However, Table 2 and Fig. 8 show that this

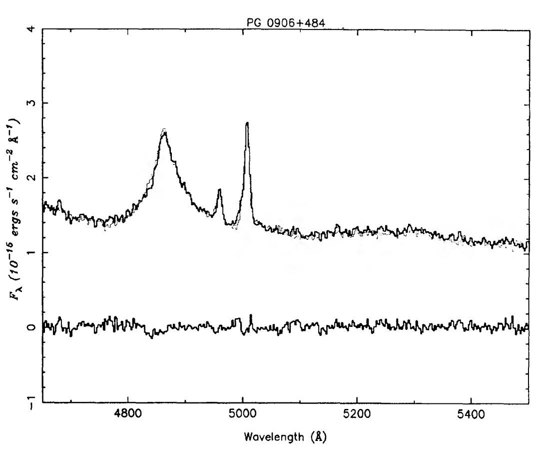

FIG. 5. The same as Fig. 1 for PG0906 + 484 (mean of JD 2447573,7572,7571 light, JD 2447848 heavy).

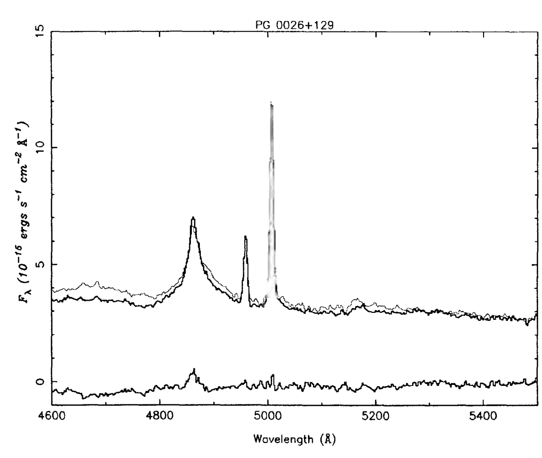

FIG. 6. The observational pair of PG0026 + 1219 (JD 2447778 light, JD2447848 heavy) and their difference.

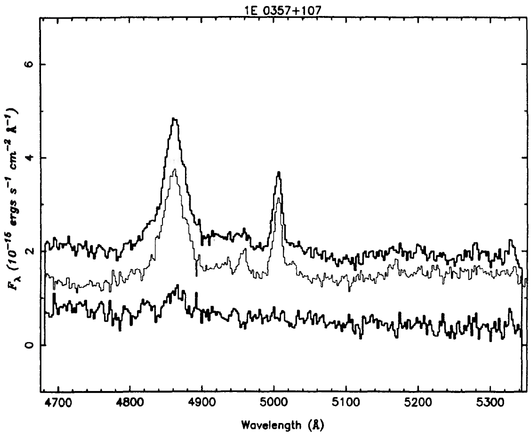

FIG. 7. The two observations of 1E0357 + 107 (JD 2447572 light, JD 2447573 heavy) and their difference.

QSO underwent very significant broad Hβ and continuum variations (+ 24% and + 25%, respectively) between a 276 day period (JD 2447573 and JD 2447849). The changes in the broad emission line and continuum are 3.4σ and 3.5σ variations, respectively. The night sky lines of [O I] $\lambda\lambda$ 6300,6363 fall near 4876 and 4925 Å, respectively. However, there is no indication of over- or undersubtraction of these lines in any of the spectra, and indeed the bulk of the residual flux lies blueward of these positions, and is as broad as either of the parent broad Hβ profiles. He II λ 4686 and/or the Bowen fluorescence line N III λ 4640 and probably broad Fe II apparently also increased in flux over the time interval. In this instance, we have no doubt that variations occurred in both the continuum and the broad emission lines; Fig. 8 is especially convincing.

4. DISCUSSION AND SUMMARY

Even with a smaller sample and lower temporal coverage than originally planned, it is significant that this variability study found definite short timescale (< 1 yr) broad emission-line variations in at least one and possibly three radio-quiet QSOs. We believe that this confirms that the broad emission lines of the higher luminosity AGN do vary and on relatively short timescales. Column 6 of Table 4 lists the estimated characteristic sizes of the BLRs of the HLAGN in this study, assuming the "standard model." The characteristic timescale for broad emission-line variability is thus expected to be $\sim R_{\rm BLR}/c$ (note, however, that accurate predictions need to be carried out with a photoionization model for a specific AGN). In the case of 1E0514 − 005, this is over a factor of 7 larger than the observed timescale (after taking into account a factor of $1 + z$). This is similar to the situation with the better-studied lower-luminosity Seyfert 1 galaxies (see, for example, Peterson 1988). We note here that although the amplitude for broad emission line variability was measured to be rather small (~ 16%–24%), we believe that the whole BLR was responding, as the amplitudes for continuum variability were comparable to those of the emission lines. This argument assumes that the continuum-emission line process is not highly nonlinear.

Short timescale variability is certainly not rampant among the radio-quiet QSOs as only one > 3σ broad emission-line change is detected. The sample of 6 OVVQs observed by Perez *et al.* (1989) appear to be more variable than the radio-quiet QSOs selected here, for example. However, they suggest that an ionizing continuum beamed near our line of sight could account for the short timescale broad emission-line variability observed in some radio-loud QSOs and perhaps all AGN. Although there is no evidence for beamed continua in the BLRs of radio-quiet QSOs, such as those selected in our study, this possibility must be considered. Comparisons of broad emission-line variability in larger samples of OVVQs, "normal" steep and flat spectrum radio-loud QSOs, and radio-quiet QSOs of comparable luminosities might indicate to what extent the ionizing continuum incident upon the BLR gas is beamed in high luminosity AGN.

Further studies are needed to better establish what temporal sampling would be sufficient in future monitoring programs to determine the transfer functions of the BLRs (see Blandford & McKee 1982) in the high-luminosity AGN (variability studies of Seyfert galaxies are leading to the derivation of the transfer functions in some of these objects; see Maoz *et al.* 1991; Krolik *et al.* 1991; Horne *et al.* 1991).

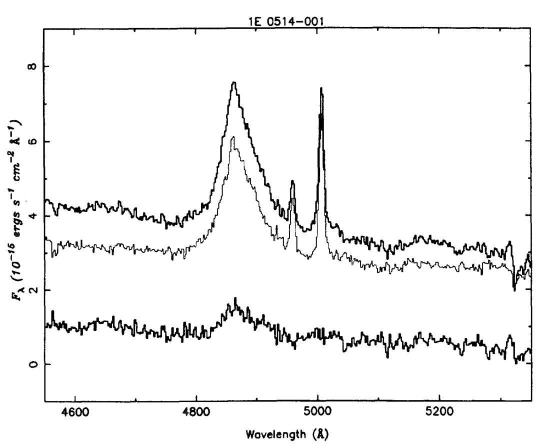

FIG. 8. The observational pair of 1E0514 − 005 (mean of JD 2447573,7560 light, JD 2447849 heavy) and their difference.

TABLE 4. Expected characteristic sizes of the BLRS from the standard model.

QSO (1)	m_V (2)	A_V[a] (3)	$-M_V$[b] (4)	log Q(H)[c] (5)	R_{BLR}(light-days)[d] (6)
PG0026+129	14.78	-	24.2	56.1	890
PG0052+251	15.42	-	23.9	56.0	790
PG0157+001	15.69	-	24.2	56.1	890
NAB0205+024	15.40	-	24.4	56.2	1000
1E0357+107	16.78	0.29	23.4	55.9	700
1E0514-005	16.18	0.38	25.5	56.6	1580
0833+446	15.60	0.10	25.4	56.6	1580
PG0906+484	16.06	-	23.1	55.7	560

[a]: Galactic extinction in magnitudes (Burstein and Heiles 1982)

[b]: Veron-Cetty, M.-P. and Veron, P. (1989); including A_V when applicable

[c]: Assuming the "mean" AGN continuum of Mathews and Ferland (1987)

[d]: Assumptions: ionization parameter, U = 0.02
hydrogen density, log n_H = 9.5 cm^{-3}

The author gratefully acknowledges the guidance of and informative discussions with B. M. Peterson, informative discussions with P. J. McCarthy and R. J. Weymann. J. A. Baldwin is also thanked for his input in the early stages of this project. This work was part of the author's doctoral dissertation submitted in partial fulfillment of degree requirements at the Ohio State University.

REFERENCES

Baribaud, T., and Alloin, D. 1990, A&A, 236, 346
Blandford, R., and McKee, C. 1982, ApJ, 255, 419
Burstein, D., and Heiles, C. 1982, AJ, 87, 1165
Byard, P. L., Foltz, C. B., Jenkner, H., and Peterson, B. M. 1981, PASP, 93, 147
Gondhalekar, P. M. 1987, in Emission Lines in Active Galactic Nuclei: Proceedings of the Sixth Rutherford Appleton Laboratory Workshop on Astronomy and Astrophysics, editor P. M. Gondhalekar, p. 214
Gondhalekar, P. M. 1990, MNRAS, 243, 443.
Gondhalekar, P. M., O'Brien, P., and Wilson, R. 1986, MNRAS, 222, 71
Heckman, T. M., Miley, G. K., van Breugel, W. J. M., and Butcher, H. K. 1981, ApJ, 247, 403
Heckman, T. M., Bothun, G. D., Balick, B., and Smith, E. P. 1984, AJ, 89, 958
Hewitt, A., and Burbidge, G. 1987, ApJS, 63, 1
Horne, K., Welsh, W. F., and Peterson, B. M. 1991, ApJL (in press)
Joly, M. 1988, A&A, 192, 87
Krolik, J., Horne, K., Kallman, T., Malkan, M., Edelson, R., and Kriss, G. 1991, ApJ, 371, 541
MacKenty, J. W., and Stockton, A. 1984, ApJ, 283, 64
Maoz, D., *et al.* 1991, ApJ, 367, 493
Mathews, W. G., and Ferland, G. J. 1987, ApJ, 323, 456
O'Brien, P. T., Zheng, W., and Wilson, R. 1989, MNRAS, 240, 741
Osterbrock, D. E. 1988, Astrophysics of Gaseous Nebulae and Active Galactic Nuclei (University Science Books, Mill Valley)
Perez, E., Penston, M. V., and Moles, M. 1989, MNRAS, 239, 75
Peterson, B. M. 1987, ApJ, 312, 79
Peterson, B. M., Foltz, C. B., and Byard, P. L. 1981, ApJ, 251, 4
Shuder, J. M. 1984, ApJ, 280, 491
Smith, E. P., Heckman, T. M., Bothun, G. D., Romanishin, W., and Balick, B. 1986, ApJ, 306, 64
Stockton, A., and MacKenty, J. W. 1987, ApJ, 316, 584
Veron-Cetty, M.-P., and Veron, P. 1989, A Catalogue of Quasars and Active Nuclei, 4th ed., ESO Science Report No. 7
Wamsteker, W., *et al.* 1990, ApJ, 354, 446
Zheng, W., and Burbidge, M. 1986, ApJL, 306, L67
Zheng, W., Burbidge, M., Smith, H. E., Cohen, R. D., and Bradley, S. E. 1987, ApJ, 322, 164